



Aza, C., Pirrera, A., & Schenk, M. (2018). Multistable Trusses of Nonlinear Morphing Elements. In J. L. Herder, & V. van der Wijk (Eds.), *2018 IEEE International Conference on Reconfigurable Mechanisms and Robots (ReMAR 2018): Proceedings of a meeting held 20-22 June 2018, Delft, Netherlands* [8449846] Institute of Electrical and Electronics Engineers (IEEE). <https://doi.org/10.1109/REMAR.2018.8449846>

Peer reviewed version

Link to published version (if available):  
[10.1109/REMAR.2018.8449846](https://doi.org/10.1109/REMAR.2018.8449846)

[Link to publication record in Explore Bristol Research](#)  
PDF-document

This is the author accepted manuscript (AAM). The final published version (version of record) is available online via IEEE at <https://ieeexplore.ieee.org/document/8449846> . Please refer to any applicable terms of use of the publisher.

## University of Bristol - Explore Bristol Research

### General rights

This document is made available in accordance with publisher policies. Please cite only the published version using the reference above. Full terms of use are available:  
<http://www.bristol.ac.uk/pure/about/ebr-terms>

# Multistable Trusses of Nonlinear Morphing Elements\*

Chrysoula Aza, Alberto Pirrera, and Mark Schenk

**Abstract**— Current compliant mechanisms rely on flexible members, whose design is often limited by strength considerations. A compliant multistable truss is introduced that consists of nonlinear morphing elements. These elements: (i) are composed of composite strips in a double-helix architecture; (ii) exhibit nonlinear stiffness characteristics; and (iii) are able to undergo large axial deformations whilst maintaining structural integrity. The overall truss behaviour can be tailored by tuning the properties of the constituent composite members, as well as the geometry of the assembled structure. This work explores the multistability of a simple truss configuration, which can provide up to five points of stable equilibrium in its range of motion.

## I. INTRODUCTION

Multistable mechanisms, *i.e.* mechanisms that are self-equilibrated in two or more stable configurations, continue to interest the research community, because they promise benefits for disparate applications, across a number of fields and length scales. To name a few examples, multistability is being investigated for use in devices such as switches, valves, precision positioning systems, reconfigurable structures, rehabilitation robotic devices, energy harvesters, and weight compensators [1-8]. An attractive feature of multistable mechanisms is that they do not require any power input to hold stable configurations, which might help save energy during operation. This characteristic can be exploited, for instance, in deployable structures that, once actuated (sometimes even passively), can self-lock in either a stowed or extended configuration [9,10]. In addition, since in general two stable equilibria will necessarily be separated by an unstable one, multistable devices present regions of negative stiffness over their work space that can be used for statically balanced mechanisms [11,12] or weight compensators [13].

It is noted that much of the literature on devices with multiple equilibria refers to bistable ones. Articles on multistability are scarcer. Oh and Kota [14] proposed the synthesis of a multistable compliant devices by combining bistable ones. In a similar manner, Han *et al.* [15] developed a quadristable mechanism, whilst tristability was achieved by Chen *et al.* [16] by employing orthogonally oriented compliant structures. The majority of these works are based on monolithic

compliance, *i.e.* the ability to transfer motion, force or energy is achieved through elastic deformations of the underlying components, rather than the mobility of joints [17]. While this may offer the possibility to achieve multistability [18], the complexities involved often result in high stresses being developed, thus posing strength limits to the potential design configurations and, consequently, the capabilities obtainable [16].

This work proposes the use of morphing composite structures as the flexible elements in a compliant truss-like mechanism. Morphing structures are able to change shape and undergo large deformations while maintaining load carrying capability and structural integrity [19]. Herein, the composite structure of double-helix architecture developed by Lachenal *et al.* [20] is used. These helical DNA-like structures, beyond variable geometry, exhibit tailorable nonlinear stiffness characteristics. This tailorability enables the ensuing mechanism to be tuned to feature a variety of responses, and a wide range of potential behaviours to be developed. The proposed truss-like mechanism may be used either on its own or as the unit cell in lattice structures [21,22].

For the sake of illustration, to present the family of possible new mechanisms conceptually arising from the ideas put forward in this paper, we focus on a simple structure resembling a von Mises truss. This structure serves as a well-known reference for the study of nonlinear, compliant mechanisms and their stability. In the following sections, we first introduce the compliant mechanism and its constituent morphing elements. Multistability is then explored using both an energy approach and a path-following method to trace equilibrium branches in force-displacement space. Conclusions and final remarks are then drawn in the last section.

## II. TRUSSES OF NONLINEAR ELEMENTS

### A. Assembly of the Mechanism

The compliant mechanism depicted in Fig. 1 consists of nonlinear composite elements with a double-helix architecture, which are described in the next subsection. This modified von Mises truss is pin-jointed at the apex and base supports. In its initial configuration, the mechanism has height  $H_0$  and its members, of length  $L_{0,i}$  and with nonlinear axial stiffness  $k_i$ , are inclined at an angle  $\alpha_{0,i}$  with respect to the horizontal. An external load is applied at the apex and the point is free to move horizontally and vertically by  $v_h, v_v$ .

### B. Constituent Double-Helix Element

Fig. 2 shows the helical geometry of the morphing elements of the truss. Each of the elements consist of two carbon fibre

\*This work was supported by the Engineering and Physical Sciences Research Council through the EPSRC Centre for Doctoral Training in Advanced Composites for Innovation and Science [grant number EP/L016028/1] and through the EPSRC Fellowship titled *Structural Efficiency and Multi-Functionality of Well-Behaved Nonlinear Composite Structures* [grant number EP/M013170/1].

C. Aza, A. Pirrera, and M. Schenk are with the Bristol Composites Institute, Advanced Composite Collaboration for Innovation and Science, University of Bristol, Bristol, BS8 1TR, UK (corresponding author phone: +44 (0) 7849238889; e-mail: chrysoula.aza@bristol.ac.uk, e-mail: alberto.pirrera@bristol.ac.uk, e-mail: m.schenk@bristol.ac.uk).

reinforced plastic strips of dimensions  $L \times W$ , connected by rigid spokes. The spokes maintain the strips at a constant distance  $H=2R$ , where  $R$  is the radius of an underlying cylinder, upon which the deformed strips can be assumed to lie [20,23]. A pre-stress is introduced in the strips by manufacturing them on a cylindrical mould of radius  $R_i$  and subsequently flattening them to form the double-helix. The double-helix is able to twist under the application of an axial force at its ends, which results in large axial displacements. The structure can deform from a straight to a completely coiled configuration, defined by the angle  $\theta \in [0^\circ, 90^\circ]$  of the helix [19]. The helical structure can be tailored to provide customizable stiffness and strain energy profiles through appropriate selection of various design parameters, such as lay-up of the strips, pre-stress and geometry [20]. The helix itself can be designed to be bistable. The initial length  $L_{0,i}$  (see Fig. 1) is the dimension of the double-helix in its extended equilibrium position.

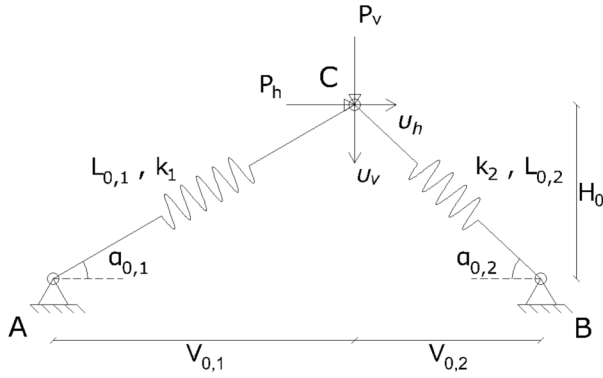
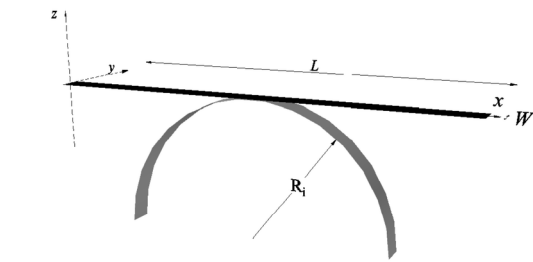
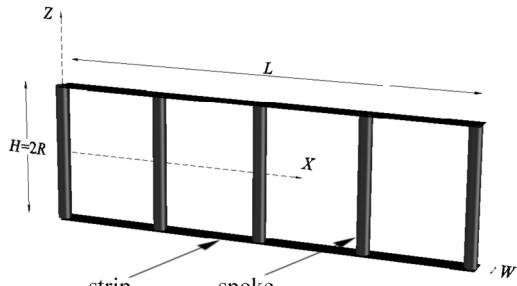


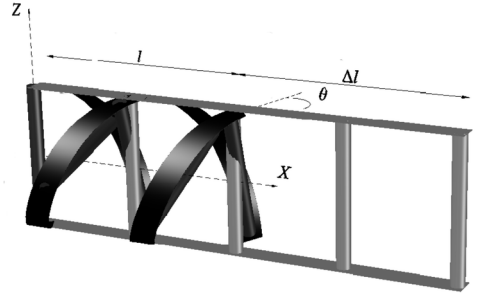
Figure 1. Schematic representation of the assembly of double-helices in a truss-like configuration.



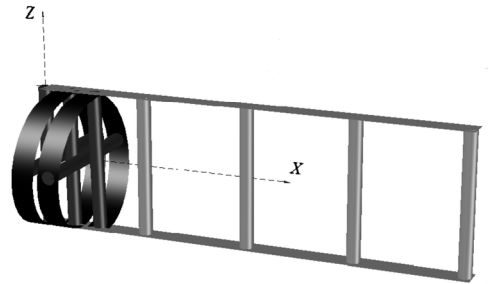
a)



b)



c)



d)

Figure 2. a) Flattening of the initially curved strips; b) fully extended configuration; c) twisted at  $\theta = 50^\circ$  (dark) and fully extended (light grey) configurations; d) fully coiled at  $\theta = 90^\circ$  (dark) and fully extended (light grey) configurations of the double-helix composite structure.

### III. ANALYSIS

Two different approaches are employed to analyse the mechanism. First, we use an energy approach to identify the stable configurations of the truss at either global or local minima of the strain energy across the mechanism's work space. Next, a path-following method is applied, for a specific load case, to obtain potential load paths between stable states.

#### A. Energy Approach

Plotting energy landscapes is an effective way to represent and characterize the behaviour of a compliant mechanism over its work space. Herder [24] and Radaelli *et al.* [25] have used potential energy landscapes to design statically-balanced structures. Here, stable and unstable equilibria of the truss are identified by inspection of the strain energy landscape. For the proposed compliant mechanism, the total strain energy is uniquely determined by the position of the end effector (*i.e.* the apex), and is the sum of the strain energy of the constituent helical members.

The strain energy,  $U$ , of each helix can be calculated analytically using the model developed by Lachenal *et al.* [19,20]:

$$U = \frac{n}{2} \int_0^L \int_{-W/2}^{W/2} [\epsilon^0]^T \begin{bmatrix} A & B \\ B & D \end{bmatrix} [\epsilon^0] dx dy, \quad (1)$$

where  $n$  is the number of strips constituting the structure,  $\epsilon^0$  are the mid-plane strains—noting that uniform mid-plane deformations are assumed—and  $\Delta \kappa$  are the changes in curvature, both referring to the local coordinate system of the strips. **A**, **B** and **D** are the in-plane, bending-extension coupling and bending stiffness matrices defined by Classical Laminate Theory [26].

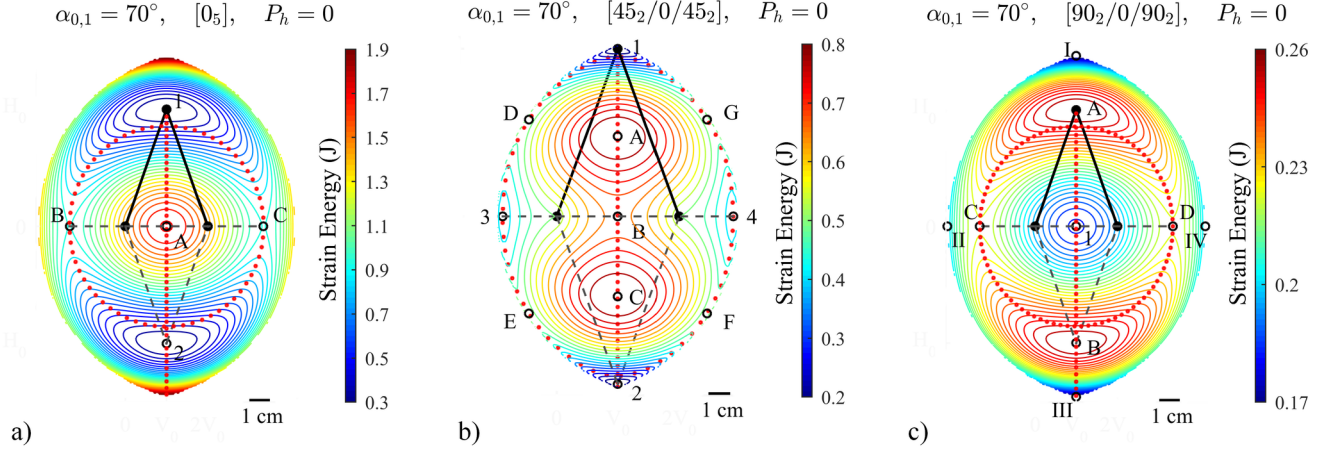


Figure 3. Strain energy landscapes for a compliant mechanism of identical double-helices of  $L = 95$  mm,  $R = 15$  mm,  $R_i = 30$  mm,  $W = 5$  mm assembled in a truss-like configuration with an initial angle  $\alpha_{0,1} = 70^\circ$  for composite strips of a  $[\beta_2/0/\beta_2]$  lay-up. The position of the truss apex under an applied vertical load ( $P_h = 0$ ) is superimposed. a)  $[0_5]$ ; b)  $[45_2/0/45_2]$ ; c)  $[90_2/0/90_2]$ . Points labelled 1–4 denote stable equilibria, while points A–G identify positions of unstable equilibrium. Points I–IV denote stable boundary equilibria. Red points indicate the equilibrium paths of the apex under the application of a vertical load.

### B. Path-following Method

Given the nonlinear nature of the system under consideration, and our interest in its stability characteristics, a path-following method is used to perform analyses in force-displacement space. This method allows one to trace stable and unstable equilibrium branches and to examine typical nonlinear behaviours, such as snap-through and snap-back, readily [15,27]. Specifically, the modified-Riks method developed by Crisfield [28] is employed here. Additionally, bifurcations and limit points are detected by inspecting the eigenvalues of the system's tangential stiffness matrix. Branch switching is realised by perturbing the structure at the bifurcation points using the respective eigenvectors [29,30]. The stability of each point along the paths is characterised by its eigenvalues, with negative eigenvalues indicating instability.

## IV. RESULTS AND DISCUSSION

Results focus on the stability analysis and characterisation of the truss-like compliant mechanism. The influence of design parameters, such as the initial geometry of the truss configuration and the lay-up of the composite strips of the constituent double-helices are explored. First, the strain energy landscapes for a steep truss comprising double-helices with different composite lay-ups are investigated. Next, their response under a vertical applied load is studied. Finally, these results are compared with those for trusses with smaller initial base angles.

### A. Effect of Composite Lay-up

The properties of the double-helices are tailored by varying the lay-up of its composite strips. Here, only symmetric lay-ups of five plies of the form  $[\beta_2/0/\beta_2]$  are considered, where  $\beta$  is the ply angle with respect to the longitudinal axis of the strip such that the zero ply angle corresponds to the  $x$ -axis of the strip in Fig. 2a. The values of  $\beta$  adopted herein are representative and selected to illustrate characteristic features of the mechanism of nonlinear element. Fig. 3 depicts the strain energy landscape of the assembled structure in a steep truss

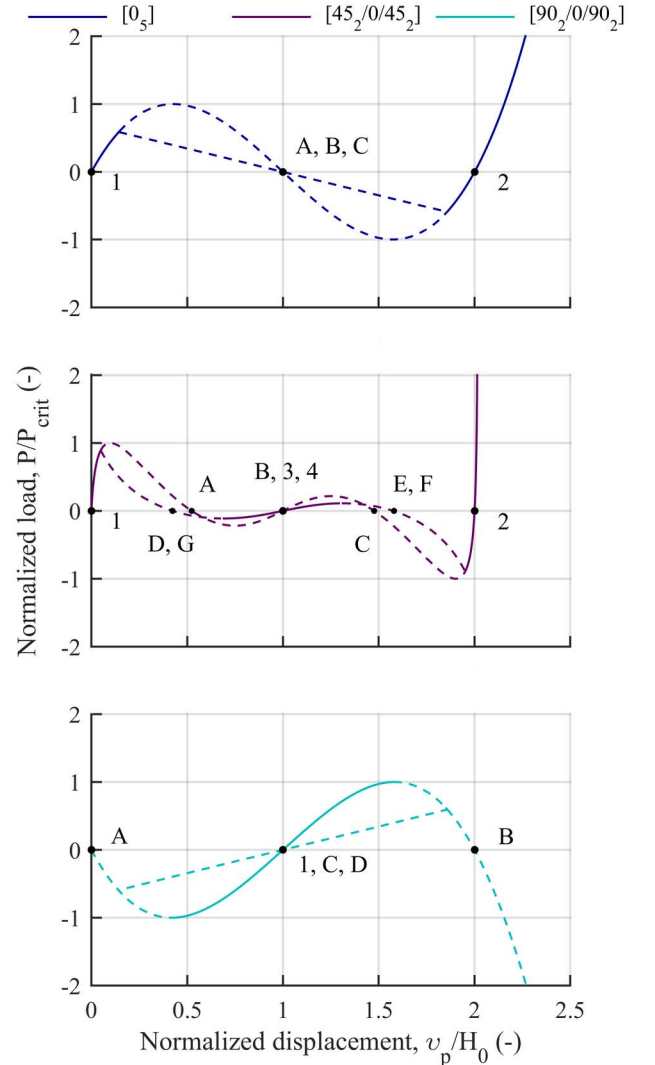


Figure 4. Load-displacement curves of the truss for different lay-ups, under the application of a vertical load at the apex. Points 1–4 are stable equilibrium points. Points A–G are unstable equilibrium points. Dashed lines represent areas of instability.

( $\alpha_{0,1} = 70^\circ$ ). Equilibrium configurations, both stable (energy minima) and unstable (energy maxima), are labelled with Arabic numbers and letters, respectively. Stable equilibria found on the boundary of the landscape are labelled with Roman numbers. Laminate lay-up affects the stability characteristics of the assembly, which can exhibit up to five stable configurations.

For  $\beta = 0^\circ$  the truss is bistable, with stable states in the initial configuration and at a vertical displacement of  $2H_0$  (points 1 and 2 in Fig. 3a). The mechanism exhibits a single internal stable equilibrium state for a  $[90_2/0/90_2]$  lay-up, when the two double-helices are collinear (point 1 in Fig. 3c), while an additional four boundary equilibria can be identified (points I–IV in Fig. 3c), making this configuration of the mechanism pentastable. For all other ply angles,  $0^\circ < \beta < 90^\circ$ , the assembly is quadristable; these equilibrium positions are marked as points 1–4 in Fig. 3b.

The mechanism's force-displacement response upon application of a vertical load at the apex is presented in Fig. 4. The apex positions are superimposed on the strain energy plots in Fig. 3. A bifurcation of the equilibrium path is present in all cases, resulting in both horizontal and vertical displacements of the apex. The bifurcated branches enable the mechanism to

deform to all the possible internal equilibrium configurations identified on the strain energy landscape just by applying a vertical load at the apex.

A closer inspection of the strain energy landscape for double-helices with symmetric  $[\beta_2/0/\beta_2]$  lay-ups, with  $0^\circ < \beta < 90^\circ$ , reveals additional features of interest. Consider the strain energy profile along the vertical passing through the apex, plotted in Fig. 5a for  $\beta = 45^\circ$ . Along this path, the strain energy exhibits three valleys (minima), suggesting stable equilibrium configurations at points 1, B and 2. However, from inspection of the energy landscape, point B is unstable. This instability is also identified in the path-following algorithm by a negative eigenvalue for the horizontal displacement. Nonetheless, point B can be stabilised under application of a vertical load by constraining lateral displacement of the apex ( $v_h = 0$ ), which also removes lateral bifurcation paths (Fig. 5b). Under these conditions the assembly of double-helices can be considered tristable.

### B. Effect of Initial Truss Angle

Next, the effect of initial truss geometry on the mechanism's behaviour is explored. Fig. 6 presents the strain energy landscapes for truss configurations with different initial angles  $\alpha_{0,1}$  and with a fixed  $[45_2/0/45_2]$  strip lay-up.

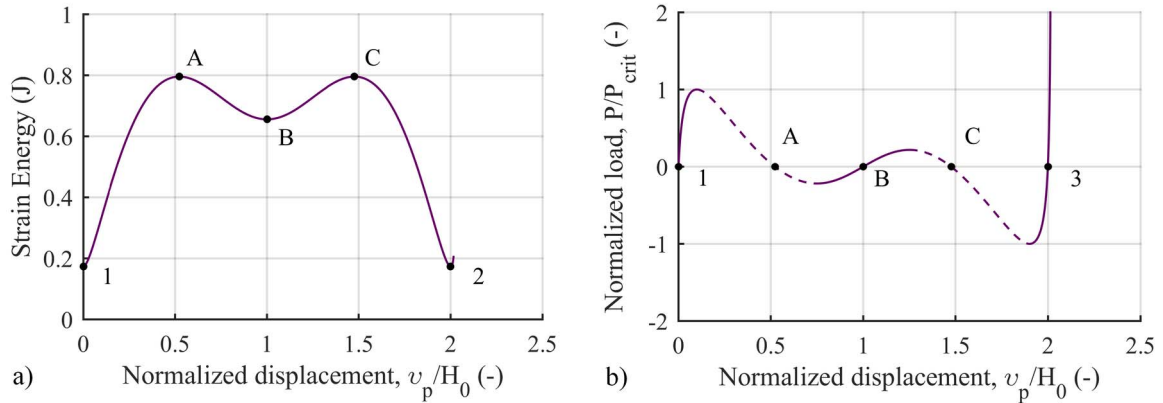


Figure 5. a) Strain energy profile along the vertical line passing through the apex for a mechanism of double-helices with a  $[45_2/0/45_2]$  lay-up,  $L = 95$  mm,  $R = 15$  mm,  $R_i = 30$  mm and  $W = 5$  mm, assembled in a truss-like configuration and with an initial base angle  $\alpha_{0,1} = 70^\circ$ ; b) Associated load-displacement curve derived by applying a vertical load at the apex, while constraining its lateral displacement ( $v_h = 0$ ). Under these conditions points 1, 3 and B are stable equilibrium points; points A and C are unstable equilibrium points. Dashed lines represent areas of instability.

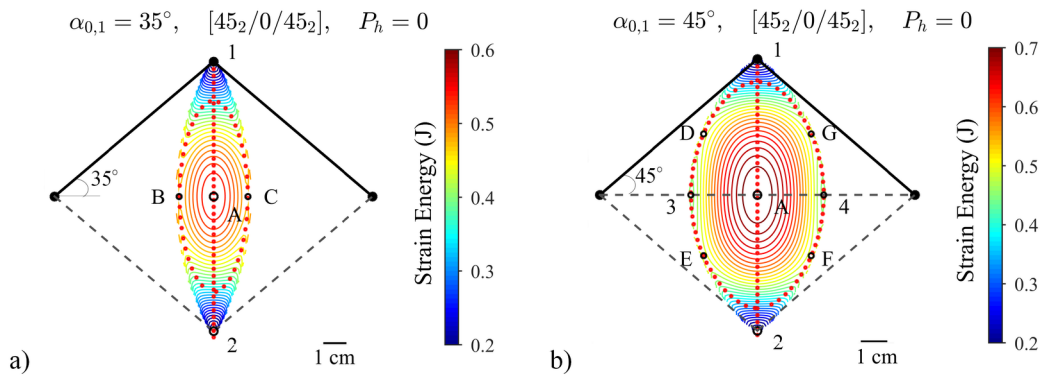


Figure 6. a) Strain energy landscape for a compliant mechanism of identical double-helices with a  $[45_2/0/45_2]$  composite strip lay-up,  $L = 95$  mm,  $R = 15$  mm,  $R_i = 30$  mm,  $W = 5$  mm, assembled in a truss-like configuration with initial base angles a)  $\alpha_{0,1} = 35^\circ$ , and b)  $\alpha_{0,1} = 45^\circ$ . Points 1–4 denote stable equilibrium positions, while points A–G indicate positions of unstable equilibrium. The position of the truss apex under an applied vertical load ( $P_h = 0$ ) is superimposed as red points.



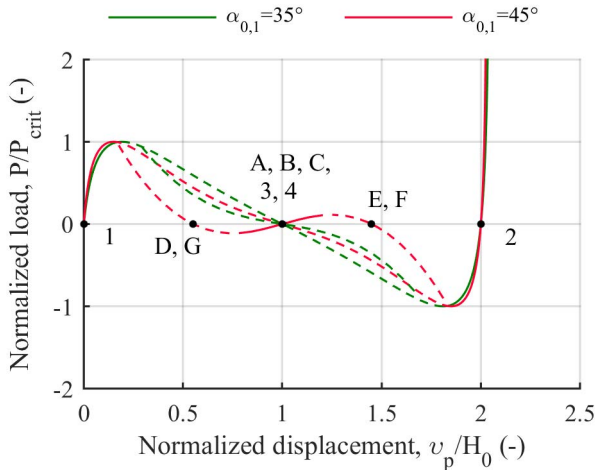


Figure 7. Load-displacement curves of a mechanism of different initial truss angles  $\alpha_{0,1}$  consisting of double helices of  $[45_2/0/45_2]$  layout,  $L = 95$  mm,  $R = 15$  mm,  $R_t = 30$  mm,  $W = 5$  mm under the application of a vertical load at the apex. Points 1–4 are stable equilibrium points. Points A–G are unstable equilibrium points. Dashed line represents the areas of instability.

The initial truss geometry affects the energy landscapes, and thereby the stability characteristics of the compliant mechanism. For a shallow truss with  $\alpha_{0,1} = 35^\circ$ , a total of five equilibrium positions are identified, of which two are stable (marked as points 1 and 2 in Fig. 6a). In a steeper truss with  $\alpha_{0,1} = 45^\circ$ , four stable configurations are found, out of a total of nine equilibrium positions (marked as points 1–4 in Fig. 6b). Thus, the mechanism, assembled in a shallow truss is bistable, while in a steeper truss it can be quadristable.

Fig. 7 presents the load-displacement curves under a vertical applied load at the apex ( $P_h = 0$ ). The corresponding positions of the apex are superimposed on the strain energy plots in Fig. 6. In both cases, a bifurcation of the equilibrium path occurs, with the apex experiencing both horizontal and vertical displacements, thereby connecting all possible equilibria. For a shallow truss ( $\alpha_{0,1} = 35^\circ$ ) the bifurcated branch is unstable along its whole range, compared to steeper trusses ( $\alpha_{0,1} = 45^\circ$  or  $70^\circ$ ) where a region of stability exists.

## V. CONCLUSIONS

A new mechanism consisting of morphing elements with tailorable nonlinear stiffness is presented. The ensuing nonlinear behaviour and multistability of the system are explored. The proposed mechanism could be used either on its own or as a building block in a lattice structure. Its behaviour can be tailored by tuning global geometric parameters and/or the characteristics of the double-helices themselves.

The response of the mechanisms is analysed globally by inspecting its potential (strain) energy landscape; peaks and valleys corresponding to unstable and stable equilibria, respectively. The mechanism's multistability characteristics are investigated parametrically by varying the lay-up of the composite strips composing the double-helices and the initial truss geometry. Quadristable behaviour is obtained for steep trusses and symmetric composite lay-ups of the form  $[\beta_2/0/\beta_2]$ , with  $0^\circ < \beta < 90^\circ$ . For  $\beta = 0^\circ$  and  $\beta = 90^\circ$ , the mechanism

becomes bistable and pentastable, respectively. Similarly, the mechanism transitions from being quadristable to being bistable for decreasing initial truss angles. Responses in load-displacement space are investigated by path-following equilibrium branches. Interestingly, via application of a vertical load, a path is found that connects all internal equilibria of the trusses. Future work will aim to investigate the manufacturability of the proposed compliant mechanism.

## REFERENCES

- [1] G. Chen, S. Zhang, G. Li, "Multistable behaviors of compliant Sarrus mechanisms," *J. Mech. Robot.*, vol. 5, pp. 021005-1–021005-10, May 2013.
- [2] G. Chen, Y. Gou, and L. Yang, "Research on Multistable Compliant Mechanisms: The State of the Art," in *Proc. 9th Int. Conf. Frontiers of Design and Manufacturing*, Changsha, China, 2010.
- [3] D. L. Wilcox, and L. L. Howell, "Fully Compliant Tensural Bistable Micro-mechanisms (FTBM)," *J. Microelectromech. Syst.*, vol. 14, no. 6, pp. 1223-1235, Dec. 2005.
- [4] Y. H. Hu, K. H. Lin, S. C. Chang, and M. Chang, "Design of a Compliant Micromechanism for Optical-Fiber Alignment," *Key Eng. Mat.*, vols. 381-382, pp. 141-144, Jan. 2008.
- [5] T. G. Nelson, R. J. Lang, N. A. Pehrson, S. P. Magleby SP, and L. L. Howell, "Facilitating Deployable Mechanisms and Structures Via Developable Lamina Emergent Arrays," *J. Mech. Robot.*, vol. 8, no. 3, pp. 031006-1–031006-10, Mar. 2016.
- [6] E. Sung, A. H. Slocum, R. Ma, J. F. Bean, and M. L. Culpepper, "Design of an Ankle Rehabilitation Device Using Compliant Mechanisms," *J. Med. Device*, vol. 5, no. 1, pp. 011001-1–011001-7, Jan. 2011.
- [7] S. P. Pellegrini, N. Tolou, M. Schenk, and J. L. Herder, "Bistable vibration energy harvesters: A review," *J. Intel. Mat. Syst. Str.*, vol. 24, no. 11, pp. 1303-1312, Jul. 2013.
- [8] A. D. Shaw, S. A. Neild, D. Wagg, P. M. Weaver, and A. Carrella, "A nonlinear spring mechanism incorporating a bistable composite plate for vibration isolation," *J. Sound Vib.*, vol. 332, no. 24, pp. 6265-6275, Nov. 2013.
- [9] A. D. Norman, S. D. Guest, and K. A. Seffen, "Novel Multistable Corrugated Structures," in *Proc. 48th AIAA/ASME/ASCE/AHS/ASC Structures, Structural Dynamics and Materials Conf.*, Waikiki, Hawaii, 2007.
- [10] S. A. Zirbel, K. A. Tolman, B. P. Trease, and L. L. Howell, "Bistable Mechanisms for Space Applications," *PLoS ONE*, vol. 11, no. 12, Dec. 2016.
- [11] M. Tolou, V. A. Henneken, and J. L. Herder, "Statically-Balanced Compliant Micro Mechanisms (SB-MEMS): Concepts and Simulation," in *Proc. ASME Design Engineering Technical Conf. & Computers and Information in Engineering Conf.*, Montreal, Canada, 2010.
- [12] K. Hoetmer, J. L. Herder, and C. J. Kim, "A Building Block Approach for the Design of Statically Balanced Compliant Mechanisms," in *Proc. ASME Design Engineering Technical Conf. & Computers and Information in Engineering Conf.*, San Diego, CA, 2009.
- [13] G. Chen, and S. Zhang, "Fully-Compliant Statically-Balanced Mechanisms Without Prestressing Assembly: Concepts and Case Studies," *Int. J. Mech. Sci.*, vol. 2, no. 2, pp. 169–174, Aug. 2011.
- [14] Y. S. Oh, and S. Kota, "Synthesis of multistable equilibrium compliant mechanisms using combinations of bistable mechanisms," *J. Mech. Design*, vol. 131, pp. 021002-1–021002-11, Feb. 2009.
- [15] J. S. Han, C. Muller, U. Wallrabe, and J. G. Korvink, "Design, Simulation, and Fabrication of a Quadstable Monolithic Mechanism with X- and Y- Directional Bistable Curved Beams," *J. Mech. Des.*, vol. 129, no. 11, pp. 1198-1203, Nov 2006.
- [16] G. Chen, Q. T. Aten, S. Zirbel, B. D. Jensen, and L. L. Howell, "A Tristable Mechanism Configuration Employing Orthogonal Compliant Mechanisms," *J. Mech. Robot.*, vol. 2, pp. 014501-1–014501-6, Feb. 2010.
- [17] C. J. Kim, S. Kota, and Y.-M. Moon, "An instant center approach toward the conceptual design of compliant mechanisms," *J. Mech. Des.*, vol. 128, no. 3, pp. 542-550, Jul. 2005.

- [18] L. L. Howell, *Compliant Mechanisms*, New York: Wiley, 2001.
- [19] X. Lachenal, P. M. Weaver, and S. Daynes, "Influence of transverse curvature on the stability of pre-stressed helical structures," *Int. J. Solids Struct.*, vol. 51, no. 13, pp. 2479-2490, Jun. 2014.
- [20] X. Lachenal, P. M. Weaver, and S. Daynes, "Multi-stable composite twisting structure for morphing applications," *Proc. R. Soc. A: Math. Phys. Eng. Sci.*, vol. 468, no. 2141, pp. 1230-1251, May 2012.
- [21] A. Viggliotti, and D. Pasini D, "Stiffness and strength of tridimensional periodic lattices," *Comput. Methods Appl. Mech. Engrg.*, vol. 229-232, pp. 27-43, Jul. 2012.
- [22] B. Haghpanah, L. Salari-Sharif, P. Pourrajab, J. Hopkins, and L. Valdevit, "Multistable shape-reconfigurable architected materials," *Adv. Mater.*, vol. 28, pp. 7915-7920, Jul. 2016.
- [23] L. Cappello, X. Lachenal, A. Pirrera, F. Mattioni, P. M. Weaver, and L. Masia, "Design, characterization and stability test of a multistable composite compliant actuator for exoskeletons," *5th IEEE RAS EMBS Int. Conf. Biomed. Robot. Biomechatron.*, pp. 1051-1056, 2014.
- [24] J. L. Herder, "Energy-free systems: theory, conception, and design of statically balanced spring mechanisms," PhD Thesis, University of Technology Delft, Delft, 2001.
- [25] G. Radaelli, and J. L. Herder, "A potential energy field (PEF) approach to the design of a compliant self-guiding statically-balanced straight-line mechanism," *Mech. Mach. Theory*, vol. 114, pp. 141-155, Apr. 2017.
- [26] L. P. Kollar, *Mechanics of Composite Structures*, Springer GS, Cambridge University Press, Cambridge, UK, 2003.
- [27] M. A. Crisfield, "A fast incremental/iterative solution procedure that handles "snap-through"," *Comput. Struct.*, vol. 62, pp. 55-62, 1981.
- [28] J. N. Reddy, *An Introduction to Nonlinear Finite Element Analysis: with applications to heat transfer, fluid mechanics, and solid mechanics*, 2nd Ed, Oxford University Press, 2015.
- [29] W. Wagner, and P. Wriggers, "A simple method for the calculation of postcritical branches," *Eng. Comput.*, vol. 5, pp. 103-109, 1988.
- [30] P. Wriggers, and J. C. Simo, "A general procedure for the direct computation of turning and bifurcation points," *Int. J. Numer. Meth. Eng.*, vol. 30, pp. 155-176, 1990.